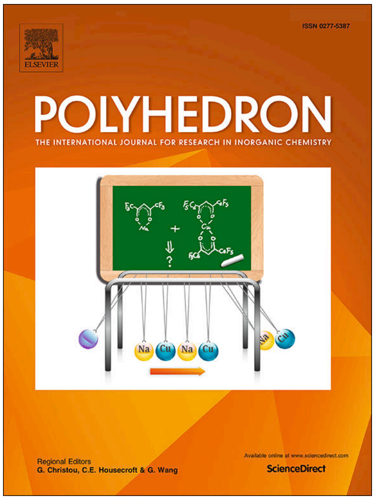

Catalytic and stoichiometric oxoiron(IV) assisted oxidation of hydrocynnamaldehyde under air

Flóra Viktória Csendes, József Kaizer

PII: S0277-5387(20)30162-5
DOI: https://doi.org/10.1016/j.poly.2020.114505
Reference: POLY 114505

To appear in: *Polyhedron*

Received Date: 22 January 2020
Accepted Date: 7 March 2020

Please cite this article as: F. Viktória Csendes, J. Kaizer, Catalytic and stoichiometric oxoiron(IV) assisted oxidation of hydrocynnamaldehyde under air, *Polyhedron* (2020), doi: https://doi.org/10.1016/j.poly.2020.114505

Catalytic and stoichiometric oxoiron(IV) assisted oxidation of hydrocynnamaldehyde under air

Flóra Viktória Csendes and József Kaizer[*]

[a]*Department of Chemistry, Universtiy of Pannonia, 8201 Veszprém, Hungary*

Abstract

Nonheme iron(II) complexes, $[(N4Py)Fe^{II}(CH_3CN)](ClO_4)_2$ (**1**) and $[(N4Py^*)Fe^{II}(CH_3CN)](ClO_4)_2$ (**2**) with pentadentate tetrapyridyl ligands (N4Py = *N*,*N*'-bis(2-pyridylmethyl)-*N*-bis(2-pyridyl)methylamine, N4Py* = *N*,*N*-bis(2-pyridylmethyl)-1,2-di(2-pyridyl)ethylamine) have been shown to catalyze the oxidation of hydrocinnamaldehyde (HCA) with H_2O_2 under air resulting hydrocinnamic acid as the predominant product with phenylacetaldehyde, phenethyl alcohol and benzaldehyde side-products as a result of a free-radical chain process via the formation of reactive phenylpropionyl radical and its consecutive reaction with molecular oxygen. The stoichiometric oxidation of HCA with in situ generated high-valent oxoiron(IV) species under air was also investigated and based on the catalytic and stoichiometric results plausible mechanism including free radical process and high-valent intermediate (Fe^{IV}=O) with rebound and non-rebound routes was proposed.

Keywords: Bioinspired oxidation, C-H activation, Oxidative cleavage, Nonheme oxoiron(IV) complex, Kinetics.

1. Introduction

The oxidation and oxidative cleavage products of hydrocinnamaldehyde (HCA) such as hydrocinnamic acid and phenylacetaldehyde are important organic chemicals for food, pharmaceutical and chemical industries [1-3]. Hydrocinnamic acid is used in the preparation of pharmaceuticals, including Rosagiline and other protease inhibitors used in the treatment of Parkinson's disease and HIV, respectively [4], while phenylacetaldehyde is responsible for the antibiotic activity of maggot therapy [5]. As natural sources, hydrocinnamic acid is a substrate of the enzyme oxidoreductases [EC 1.14.12.19] in the pathway of phenylalanine metabolism [6-8], and phenylacetaldehyde can be also biosynthetically derived from the phenylalanine [9]. The oxidation of aldehydes to give carboxylic acids has been reported using stoichiometric reagents such as Cr(IV)-based Jones [10-11], the Ag(I)-based Tollen's

---

[*] Corresponding author. Tel.: +36 88 62 4720; Fax: + 36 88 62 4469.
E-mail address: kaizer@almos.uni-pannon.hu.

[12], the Cu(II)-based Fehling's [13], and permanganate reagents[14]. Carboxylic acids such as hydrocinnamic acid can be also obtained by the heterogeneous catalytic aqueous-phase oxidation of aldehydes using silver(I)/copper(II) oxide [15], and by homogeneous catalytic oxidation of aldehyde using water-soluble N-heterocyclic carbene- and a silver(I)-catalyst with oxygen in water [16-17]. Phenyl acetaldehyde can be obtained e.g. by Wacker oxidation of styrene [18-20] and dehydrogenation of 2-phenylethanol with silver or gold catalysts [21].

Synthetic iron complexes as model catalysts of nonheme oxidase and oxygenase enzymes, have been widely used for the selective oxidation (oxygenation) of hydrocarbons, alcohols, alkenes, aldehydes and sulfides, where in general high-valent iron-oxo ($Fe^{IV}=O$ or $Fe^{V}=O$) intermediates were proposed as key metal-based oxidants [21-34]. In a series catalytic studies, e.g. oxidative *N*-dealkylation of *N*,*N*-dimethylanilines [35], epoxidation of olefins [36], and hydroxylation of ethylbenzene [37], mononuclear iron complex $[Fe^{II}(N4Py^*)(CH_3CN)](ClO_4)_2$ with chiral pentadentate ligand, N4Py* (N4Py* = *N*,*N*-bis(2-pyridylmethyl)-1,2-di(2-pyridyl)ethylamine) was shown to react with H_2O_2, generating a highly reactive high-valent nonheme iron species $[Fe^{IV}(N4Py^*)(O)](ClO_4)_2$, and non-selective hydroxyl radicals [37]. The moderate (enantio)selectivities in these systems can be explained by the non-selective radical processes including also the metal-based oxidation via radical, dissociative, non-rebound (non-RM) mechanism. In the case of the rebound mechanism (RM) the rate-determining step of the C-H bond activation is the hydrogen atom abstraction (HAA) resulting in the formation of the alkyl (acyl) radical species in the cage [$Fe^{III}OH$--•CR_2 or •C(O)R)], which is followed by a rebound of the radical to the OH moiety of the Fe^{III} intermediate, forming alcohol (carbonic acid) product in a fast step [38]. However, in the case of non-RM pathway the radical dissociates, and the leaving radical can undergo rearrangement before the rebound step, or react with O_2 at diffusion-controlled rates [38]. We have recently reported the hydroxylation of aromatic aldehydes to carboxylic acids by $[Fe^{IV}(N4Py)(O)](ClO_4)_2$ (N4Py = *N*,*N*'-bis(2-pyridylmethyl)-*N*-bis(2-pyridyl)methylamine) and $[Fe^{IV}(N4Py^*)(O)](ClO_4)_2$ complexes under argon, where the RM pathway including a rate-controlling HAA step has been established based on detailed kinetic and mechanistic results: high yield of products (Fe^{II} and $PhCO_2H$), Bell-Evans-Polanyi plot (log k_2 versus $BDE_{C\text{-}H}$, BDE = bond dissociation energy), and large kinetic isotope effect (*KIE* = 27, 37, respectively) (Scheme 1) [25]. As a continuity of this study we have choosed and investigated the stoichiometric and catalytic oxidation of arylalkyl aldehyde, hydrocinnamaldehyde (HCA) by the aforementioned $Fe^{IV}=O$ complexes and their precursor Fe^{II} complexes with H_2O_2 under air to get more insight into the mechanism (RM versus non-RM pathway) of these curious reactions.

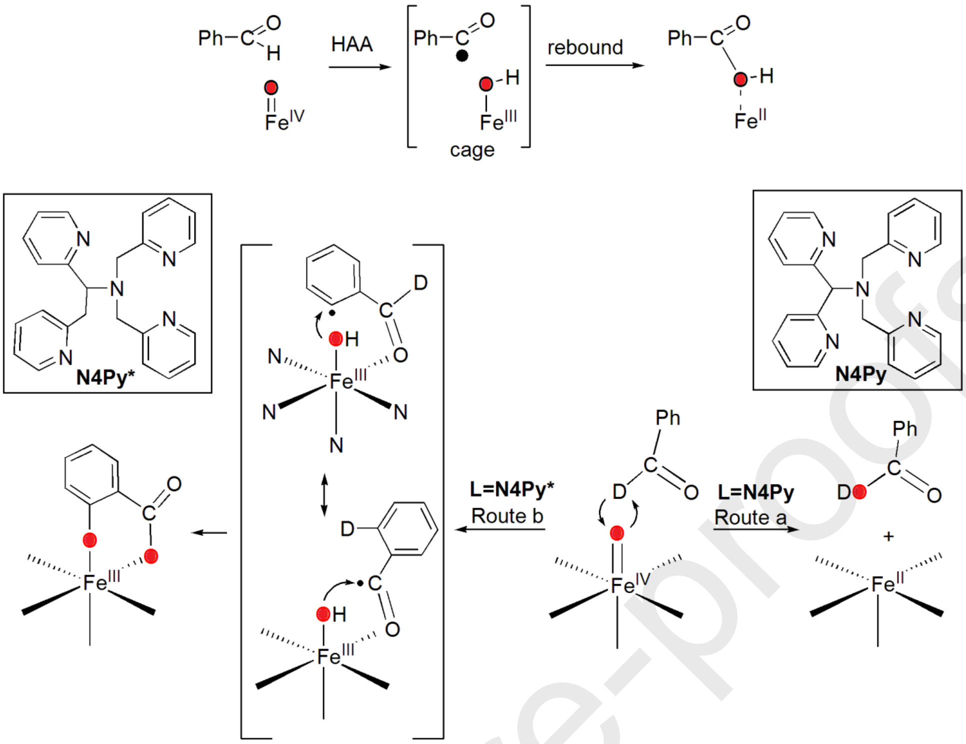

Scheme 1. Previously proposed mechanism for the stoichiometric oxoiron(IV) mediated oxidation of benzaldehyde under argon [25].

2. Experimental section

2.1. Materials and methods

The ligands N4Py and N4Py*, and their complexes $[Fe^{II}(N4Py)(CH_3CN)](ClO_4)_2$ (**1**) and $[Fe^{II}(N4Py^*)(CH_3CN)](ClO_4)_2$ (**2**) were prepared according to published procedures [27,28,39,40]. UV/Vis spectra were recorded with an Agilent 8453 diode-array spectrophotometer with quartz cells. Infrared spectra were recorded with an Avatar 330 FTIR Thermo Nicolet instrument. UV/Vis spectra were recorded with an Agilent 8453 diode-array spectrophotometer with quartz cells. Microanalyses were performed by the Microanalytical Service of the University of Pannonia and Atlantic Microlab. The consumption of the starting hydrocinnamaldehyde and formation of benzaldehyde, phenylacetaldehyde, phenethyl alcohol and hydrocinnamic acid were monitored by GC and GC-MS (Shimadzu GCMS-QP2010-SE equipped with a secondary electron multiplier detector with conversion dynode and a 30 m HP-5MS column).

2.2. Description of the catalytic oxidation reactions

In a typical reaction, 0.5 cm^3 of H_2O_2 (diluted from 35% solution) solution in CH_3CN was delivered by syringe pump in air to a stirred solution (1 mL) of catalyst **1**, **2** or $Fe(ClO_4)_2$ salt, and hydrocinnamaldehyde (HCA) substrate inside a vial. The final concentrations were 3 mM catalyst (**1**, **2** or $Fe(ClO_4)_2$), 300 mM H_2O_2, and 300 mM HCA. After syringe pump addition (10 min the solution was stirred for 5 minutes and a known amount of PhBr (150 mM) was added as an internal standard (Table 1). The iron complex was removed by passing the reaction mixture through a neutral alumina column followed by elution with ethyl acetate (0.15 cm^3). The products (benzaldehyde, phenylacetaldehyde, phenethyl alcohol and hydrocinnamic acid) were identified by GC/MS and confirmed by comparison with authentic samples. GC-MS spectra for benzaldehyde m/z: 106 (93.60 %), 105 (88.80 %), 77 (100 %), 74 (9.60 %), 52 (14.00 %), 51 (49.60 %), 39 (7.20 %), for phenylacetaldehyde m/z: 120 (15.57 %), 108 (5.82 %), 92 (29.42 %), 91 (100 %), 79 (12.75 %), 77 (9.79 %), 65 (36.14 %), 63 (23.11 %), 51 (21.60 %), 39 (38.96 %), for phenylethyl alcohol m/z: 122 (20.36 %), 92 (51.15 %), 91 (100 %), 77 (10.60 %), 65 (34.80 %), 51 (19.84 %), 39 (28.95 %), for hydrocinnamic acid m/z: 150 (38.48 %), 131 (7.60 %), 104 (43.61 %), 103 (45.66 %), 92 (24.85 %), 91 (100 %), 79 (22.39 %), 77 (57.67 %), 65 (43.65 %), 51 (48.94 %), 39 (42.45 %), for hydrocinnamic acid (Me-ester) m/z: 164 (5.47 %), 150 (26.25 %), 104 (71.12 %), 91 (100 %), 77 (60.03 %) 65 (19.32 %), 51 (41.94 %), 39 (33.08 %).

Table 1. Catalytic oxidation of hydrocinnamaldehyde (HCA) carried out by **1** and **2** with H_2O_2 in CH_3CN at 25°C under air.

[**1**] : [HCA] : [H_2O_2] (mM)^a	Yield (%)^b PhCHO	Yield (%)^b $PhCH_2CHO$	Yield (%)^b $PhCH_2CH_2OH$	Yield (%)^b $PhCH_2CH_2CO_2H$	ΣYield (%)^b
0.5 : 300 : 700	1.93	5.09	5.61	7.33	19.96
1.5 : 300 : 700	10.67	9.46	8.32	21.57	50.03
3 . 300 : 700	12.93	8.68	8.99	49.95	80.55
3 . 300 :300	10.7	8.96	10.3	17.75	47.71
3 : 300 : 200	8.56	8.33	8.82	14.12	39.83
[**2**] : [HCA] : [H_2O_2]					
1 : 300 : 700	2.12	6.02	5.02	19.43	32.59
3 : 300 : 700	7.17	7.94	5.99	36.53	57.63
3 . 300 : 300	2.46	6.60	6.62	13.25	28.93
3 . 300 : 100	1.96	3.58	3.43	7.25	16.22
[**Fe^{II}**]^c : [HCA] : [H_2O_2]					
3 . 300 : 700	0.29	0.91	0.52	0.24	1.96

[a]Reaction conditions: see Experimental section. [b]Based on substrate, calculated from the average of two independent measurements. [c]$Fe^{II} = Fe^{II}(ClO_4)_2$.

*2.3. Stoichiometric oxidation of hydrocinnamaldehyde with $[Fe^{IV}(N4Py\ or\ N4Py^*)(O)]^{2+}$ (**3** or **4**) under air*

All reactions were carried out under thermostated conditions at different temperature in 1 cm quartz cuvettes with stirring under argon. The $[Fe^{II}(N_4Py)(CH_3CN)](ClO_4)_2$ or $[Fe^{II}(N_4Py^*)(CH_3CN)](ClO_4)_2$ complex (1.00×10^{-3} M) was dissolved in acetonitrile (1.5 cm^3), then iodosobenzene (2.00×10^{-3} M) was added to the solution. The mixture was stirred for 50 minutes, and a known amount of PhBr (1 mM) was added as an internal standard then excess iodosobenzene was removed by filtration. The rate of substrate oxidation was followed by monitoring the decrease in absorbance at 705 nm (ε = 400 M^{-1} cm^{-1} for $[Fe^{IV}(N4Py^*)(O)](ClO_4)_2$ (**4**) [40]) or 695 nm (ε = 450 M^{-1} cm^{-1} for $[Fe^{IV}(N4Py)(O)](ClO_4)_2$ (**3**) [27,28]) respectively, under pseudo-first order condition of excess HCA (20-200 equiv.). The iron complex was removed by passing the reaction mixture through a neutral alumina column followed by elution with ethyl acetate (0.15 cm^3). The products (benzaldehyde, phenylacetaldehyde, phenethyl alcohol and hydrocinnamic acid) were identified by GC/MS and confirmed by comparison with authentic samples: Yields (based on Fe^{IV}) are $PhCH_2CH_2CO_2H$ (~20%), $PhCH_2CH_2CH_2OH$ (~18%), $PhCH_2CHO$ (~19%) and PhCHO (~5%).

Table 2. Kinetic data for the stoichiometric oxidation of hydrocinnamaldehyde with $[Fe^{IV}(N4Py)(O)](ClO_4)_2$ (**3**) and $[Fe^{IV}(N4Py^*)(O)](ClO_4)_2$ (**4**) complexes under air in CH_3CN (1.5 cm^3).

No.	**T (K)**	**$PhCH_2CH_2CHO$ (10^{-3}M)**	**[3] (10^{-3}M)**	**[4] (10^{-3}M)**	**k_{obs} ($10^{-2}s^{-1}$)**	**k_2 ($10^{-1}M^{-1}s^{-1}$)**
1	298	20	1		0.618±0.038	3.09±0.19
2	298	40	1		1.070±0.051	2.68±0.13
3	298	60	1		1.370±0.03	2.28±0.05
4	298	80	1		2.090±0.088	2.61±0.11
5	298	120	1		3.120±0.108	2.60±0.09
6	298	200	1		5.145±0.200	2.57±0.10
7	293	80	1		1.707±0.060	2.13±0.07
8	288	80	1		1.367±0.054	1.71±0.06
9	283	80	1		1.063±0.026	1.32±0.04

10	278	80	1		0.899±0.051	1.12±0.05
11	298	20		1	0.182±0.009	0.91±0.05
12	298	40		1	0.328±0.014	0.82±0.04
13	298	60		1	0.494±0.023	0.82±0.04
14	298	80		1	0.613±0.025	0.77±0.03
15	298	100		1	0.819±0.023	0.82±0.02
16	298	120		1	0.914±0.053	0.76±0.04
17	298	200		1	1.310±0.092	0.66±0.05
18	293	80		1	0.369±0.016	0.46±0.02
19	288	80		1	0.259±0.014	0.32±0.02
20	283	80		1	0.178±0.008	0.22±0.01
21	278	80		1	0.127±	0.16±0.01

3. Results and discussion

3.1. Catalytic oxidation of hydrocinnamaldehyde (HCA)

The catalytic activity of $[Fe^{II}(N4Py)(CH_3CN]^{2+}$ (**1**) and $[Fe^{II}(N4Py^*)(CH_3CN]^{2+}$ (**2**) was investigated in the oxidation of HCA, utilizing H_2O_2 as the co-oxidant under air. The reactions were carried out under standard catalytic conditions (1 : 100 : 100 ratio for the catalyst : co-oxidant : substrate) in CH_3CN under air at 25°C. Co-oxidant was added by syringe, and after a definite time the reaction mixture was analyzed by GC-MS (Table 1). It took less than 15 min to have about 48 and 29 % yields (based on the substrate) for complex **1** and **2**, respectively. A much lower yield was obtained for the $Fe(ClO_4)_2$ (~2 %) (Fig.1A and Table 1). In case of catalyst **1** and **2**, the oxidation reactions produced hydrocinnamic acid as expected major product with an overall yield of 17.8 and 13.3 % in addition to three minor products; benzaldehyde (11 and 2.5 %), phenylacetaldehyde (9 and 6.6 %) and phenethyl alcohol (10 and 6.6 %), respectively. Similar results have been obtained during the aerobic oxidation of phenyl acetaldehyde in the presence of cobalt and manganese acetate as catalysts [41]. Significant increase in the yields of hydrocinnamic acid was observed when the amount of catalyst (**1**, **2**) and/or H_2O_2 was increased (50 % for **1** and 36.5 % for **2**), whilst the yields of the minor products didn't changed remarkably (Fig. 1). Similarly to our previous results, $[Fe^{II}(N4Py)(CH_3CN]^{2+}$ is a far better catalyst than $[Fe^{II}(N4Py^*)(CH_3CN]^{2+}$ for the oxidation of HCA, which may be explained by the different rigidity around the metal centres.

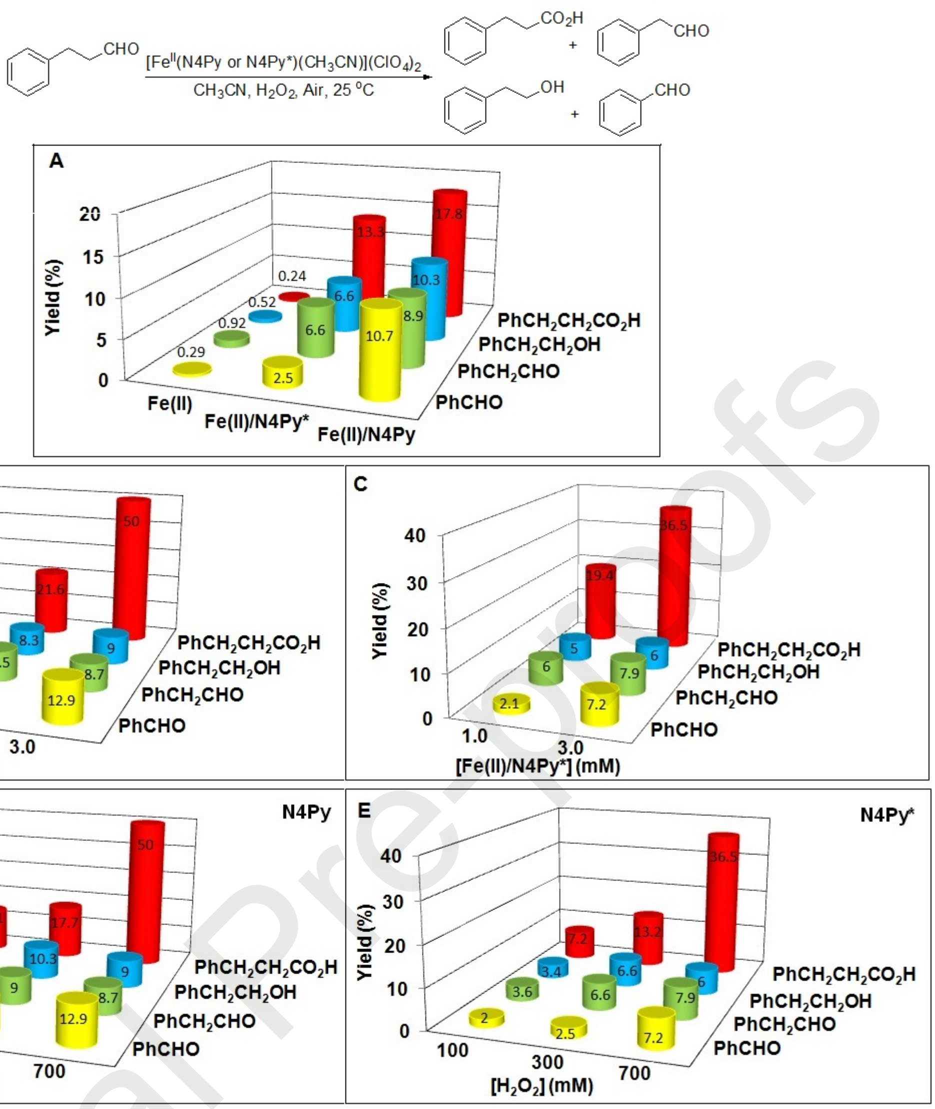

Fig. 1. (**A**) Comparison of the product formation in the iron-catalyzed ($Fe(ClO_4)_2$ vs. **1** and **2**) oxidation of hydrocinnamaldehyde with H_2O_2 as co-oxidants in CH_3CN at 25°C under air. Reaction conditions: [**Fe**, **1** or **2**]$_0$ = 3 mmol, [HCA]$_0$ = 300 mM, [H_2O_2] = 300 mM. (**B**, **C**) Effect of the amount of catalyst (**1**, **2**); [HCA]$_0$ = 300 mM, [H_2O_2] = 700 mM. (**D**, **E**) Effect of the amount of H_2O_2; [**1** or **2**]$_0$ = 3 mmol, [HCA]$_0$ = 300 mM.

The oxidative cleavage of HCA to phenylacetaldehyde (benzaldehyde) and phenethyl alcohol indicates an autooxidation process via Russel-type termination mechanism involving reactions of the $PhCH_2CH_2C(O)$• and $PhCH_2CH_2$• radicals with dioxygen to form equimolar amount of $PhCH_2CH_2OH$ and $PhCH_2CHO$ (Scheme 2) [42]. The formation of $PhCH_2CH_2C(O)$• radical may be explained either by the forming oxoiron(IV) intermediate, and the appearance of hydroxyl radical during its formation. The oxidative cleavage of HCA in the presence of oxoiron(IV) species could also occur via reaction between cage-escaped

$PhCH_2CH_2C(O)•$ radical and dioxygen. It can be concluded that the moderate selectivity can be explained by the parallel selective metal-based, and non-selective radical processes including non-RM route with oxoiron(IV) species, resulting in hydrocinnamic acid and oxidative cleaved products (consecutive products of the arylalkyl radicals formed by decarbonylation of the phenylpropionil radical), respectively. It is worth to mention that in the case of H_2O_2 the presence of dioxygen can not be excluded by the use of inert atmosphere due to the metal-based disproportionation of H_2O_2.

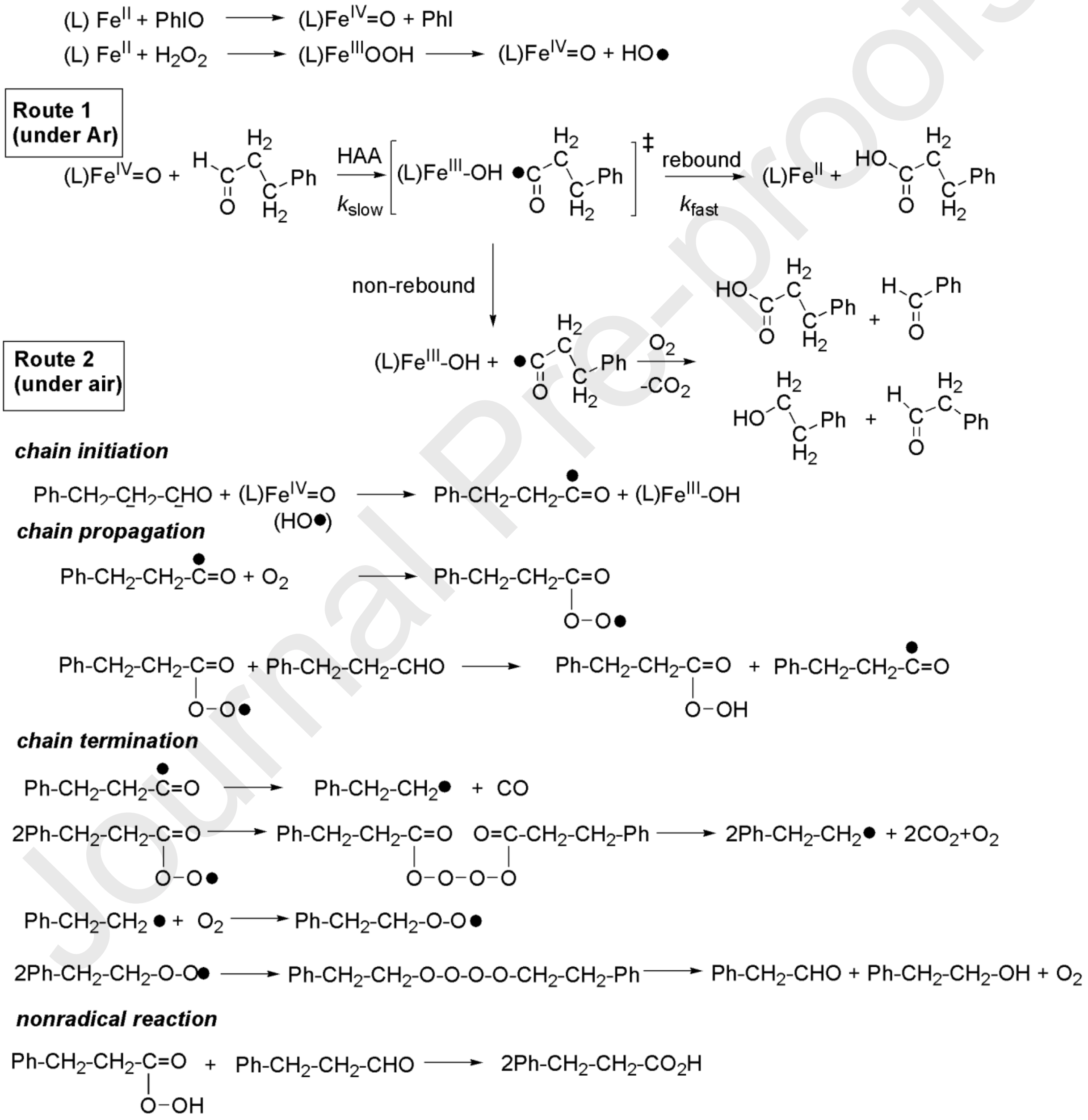

Scheme 2. Proposed mechanism in the iron(II)-catalyzed oxidation of hydocinnamaldehyde with H_2O_2 under air.

*3.2. Stoichiometric oxidation of hydrocinnameldehyde (HCA) with **3** and **4** under air*

In general free radical mechanism can be proposed for the oxidation of aldehydes with molecular oxygen in the presence of transition metal complexes such as manganese and iron, where the formation of acyl radical is the first step, which then reacts with dioxygen forming acylperoxy radical, or easily decarbonylates into alkyl radical. Previously we have found clear evidence for the formation of high-valent oxoiron(IV) species in $[Fe^{II}(N4Py^*)(CH_3CN]^{2+}/H_2O_2$-catalyzed systems. We have also found that the forming oxoiron(IV) species is capable for the oxidation of benzaldehyde to benzoic acid under argon, including rebound-type mechanism. In order to obtain more insight into the role of high-valent oxoiron(IV) intermediate on the oxidation of arylalkyl aldehydes under air, we have synthesized the oxoiron(IV) complex **3** and **4** by in situ reaction of **1** and **2** with PhIO, and investigated the stoichiometric oxidation of HCA with it under air. In this way (by the use of PhIO as an oxidant), the formation of hydroxyl radicals and its non-selective reactions can be excluded, and the possible role of the oxoiron(IV) species can be directly investigated.

The oxoiron(IV) complexes **3** and **4**, which are well-characterized iron-based oxidants with an absorbance band in the visible region (λ_{max} = 695 nm (450 M^{-1} cm^{-1}) and λ_{max} = 705 nm (400 M^{-1} cm^{-1}), respectively) were generated by reaction of **1** and **2** with PhIO in MeCN, and the rate of the decay of the absorption band at 695 nm and 705 nm was measured as a function of the concentration of added HCA (Table 2 and Fig. 2). To generate **3**, complex **1** (1 mM) was dissolved in MeCN and treated with 2 equiv of PhIO, which led to the maximum generation of **3** (~40 min), as judged by UV-vis spectroscopy, followed by a fast decomposition of the green species upon addition of HCA, which coincided with the regeneration of **1** (λ_{max} = 453 nm, 6250 M^{-1} cm^{-1}) (Fig. 2A). The yield of **1** was ~25 % at the end of the reaction of **3** with HCA based on an absorbance measurement using its extinction coefficient under these conditions. Similar result has been obtained for complex **4**. The absorption bands at 680 nm and 690 nm (~200 M^{-1} cm^{-1}) observed at the end of the reactions can be assigned to the formation of $[\{Fe^{III}(N4Py \text{ or } N4Py^*)_2\}(\mu\text{-}O)]^{4+}$ complexes from the elimination reaction of the forming $[(N4Py \text{ or } N4Py^*)Fe^{III}(OH)]^{2+}$ (~70 %) complexes. Both complexes **3** and **4** were able to oxidize the hydrocinnamaldehyde under aerobic conditions, at 25˚C in CH_3CN, and the GC/MS analysis of the products indicated the formation of hydrocinnamic acid (~20 % based on **3** and **4**), phenethyl alcohol (~18), phenylacetaldehyde (~19) and benzaldehyde (~5%). These results including the low yield of Fe(II) and hydrocinnamic acid (RM) beside the formation of $[\{Fe^{III}(N4Py \text{ or } N4Py^*)_2\}(\mu\text{-}O)]^{4+}$ and oxidative cleaved products (non-RM) are consistent with a complex system including a rebound and non-rebound mechanisms, where the dioxygen can interfere with the rebound step and results in oxidative cleaved products by reacting with the cage-leaved acyl radical. Kinetic experiments under pseudo-first-order conditions (excess of HCA) revealed 1st-order dependence on both the oxoiron(IV) species and HCA with $k_2 = 2.60 \times 10^{-1}$ M^{-1} s^{-1}, $\Delta H^{\#} = 27$ kJ mol^{-1} and $\Delta S^{\#} = -165$ J mol^{-1} K^{-1} at 298 K (Fig. 3 and Table 3). Similarly, **4** was reacted with HCA under the same conditions, and a slower rate with respect to complex **3** was obtained. The rate constant (k_2) for complex **4** was found to be $k_2 = 0.77 \times 10^{-1}$ M^{-1} s^{-1} with $\Delta H^{\#} = 51$ kJ mol^{-1} and $\Delta S^{\#} = -106$ J mol^{-1} K^{-1} at 298 K. The large negative activation entropies are typical of associative processes. Reaction rates obtained for the oxidation of HCA are 3-4 times smaller than those observed for benzaldehyde with oxoiron(IV) complexes **3** and **4** ($k_2 = 8.2 \times 10^{-1}$ and 2.2×10^{-1} M^{-1} s^{-1}, respectively [25]). Similar reaction rate values but much higher yields for hydrocinnamic acid and the Fe(II) precursor complexes (~70-80 %) were observed under argon, excluding the involvement of dioxygen in the rate-determining step.

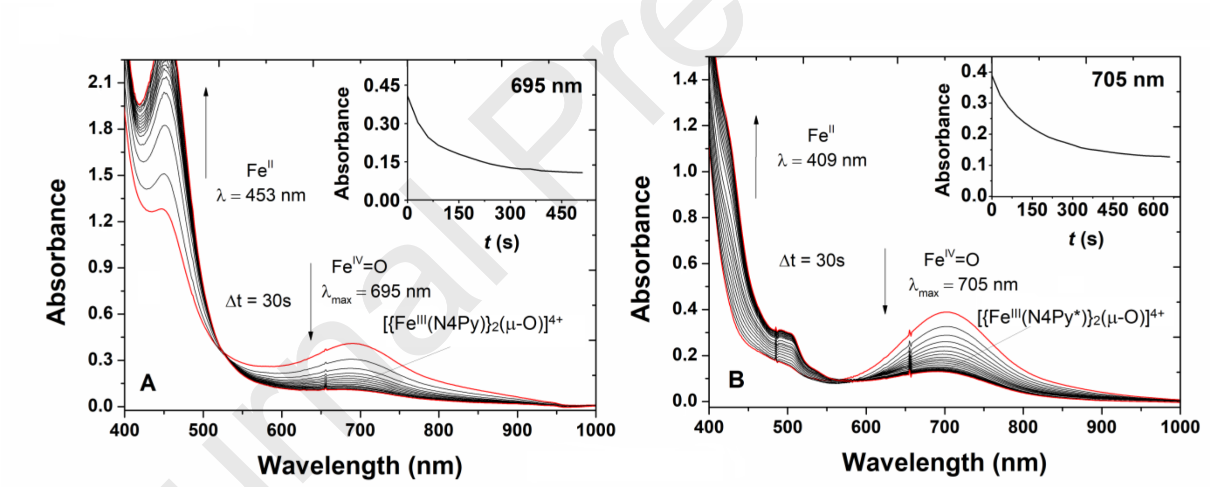

Fig. 2. Reaction of **3** and **4** (derived from the reaction of **1** and **2** with PhIO) with HCA in CH_3CN at 25°C under air: (**A**) UV-Vis spectral changes of **3** species upon addition of 60 equiv of HCA ([**3**] = 1 mM, l = 1 cm). Inset shows time course of the decay of **3** monitored at 695 nm with HCA. (**B**) UV-Vis spectral changes of **4** species upon addition of 100 equiv of HCA ([**4**] = 1 mM, l = 1 cm). Inset shows time course of the decay of **4** monitored at 705 nm with HCA.

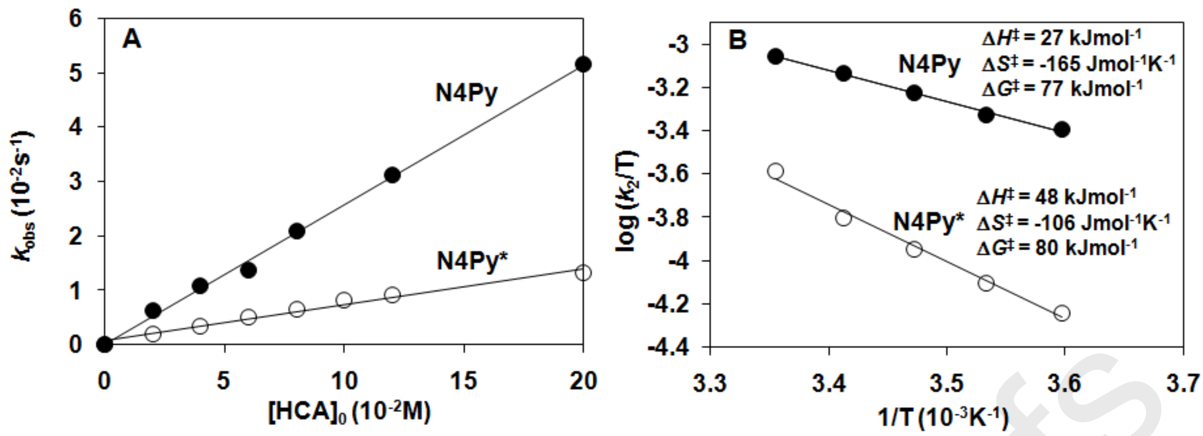

Fig. 3. Reaction of **3** and **4** (derived from the reaction of **1** and **2** with PhIO) with HCA in CH_3CN under air: (**A**) Plot of k_{obs} versus [HCA]$_0$ for reactions of **3** and **4** with HCA at 25°C ([**3** and **4**] = 1 mM). (**B**) Eyring plots of log(k_2/T) versus 1/T for the oxidation reaction of **3** and **4** with HCA ([**3** and **4**] = 1 mM, [HCA]$_0$ = 80 mM)

Table 3

Kinetic parameters determined in the oxidation of benzaldehyde and hydrocinnamaldehyde by oxoiron(IV) complexes **3** and **4** in acetonitrile at 25°C.

complex	substrate	k_2 ($M^{-1}s^{-1}$)	$\Delta H^{\neq}$ (kJmol^{-1})	$\Delta S^{\neq}$ (Jmol^{-1}K^{-1})	$\Delta G^{\neq}$ (kJmol^{-1})	Refs.
N4Py	PhCHO	8.2×10^{-1}	21	-195	79	[25]
N4Py*	PhCHO	2.2×10^{-1}	33	-168	82	[25]
N4Py	$PhCH_2CH_2CHO$	2.6×10^{-1}	27	-165	77	this work
N4Py*	$PhCH_2CH_2CHO$	7.7×10^{-2}	51	-106	80	this work

4. Summary and conclusions

Efforts have been made to work out an iron(II)-catalyzed oxidation reaction for aryl alkyl aldehyde, hydrocinnamaldehyde by the use of H_2O_2 under air, as well as their detailed mechanistic aspects. It was found that the selectivity, the product composition (hydrocinnamic acid versus oxidative cleaved products: phenylacetaldehyde, benzaldehyde and phenethyl alcohol) in both the stoichiometric and the catalytic systems remarkably depends on the presence of dioxygen. Based on experimental observations a plausible mechanism was proposed, where the high-valent oxoiron(IV) species is proposed as key oxidant in the C-H activation process via radical dissociation pathway resulting $Fe^{III}OH$ and acyl radical species. Their consecutive reactions can be explained by metal-based rebound mechanism resulting hydrocinnamic acid and non rebound free radical mechanism between the forming acyl radical and dioxygen resulting oxidative cleaved products. Based on these results we have got a further evidence for the previously proposed non-rebound mechanism.

Acknowledgements

Financial support of the Hungarian National Research Fund (OTKA K108489), and GINOP-2.3.2-15-2016-00049 are gratefully acknowledged.

References

[1] S. M. Korneev, Synthesis 45 (2013) 1000.
[2] Q. Zhou, C. L. Wintersteen, K. R. Cadwallader, J. Agric. Food Chem. 50 (2002) 2016.
[3] M. Aznar, R. Lopez, J. Cacho, V. Ferreira, J. Agric. Food Chem. 51 (2003) 2700.
[4] G. Ma, Z. Xu, P. Zhang, J. Liu, X. Hao, J. Ouyang, P. Liang, S. You, X. Jia, Org. Process Res. Dev. 18 (2014) 1169.
[5] E. R. Pavillard, E. A. Wright, Nature 180 (1957) 916.
[6] E. Diaz, A. Ferrandez, J. L. Garcia, J. Bacteriol. 180 (1998) 2915.
[7] R. Burlingame, P. J. Chapman, J. Bacteriol. 155 (1983) 113.
[8] E. Diaz, A. Ferrandez, M. A. Prieto, J. L. Garcia, Microbiol. Mol. Biol. Rev. 65 (2001) 523.
[9] J. Wouters, Curr. Med. Chem. 5 (1998) 137.
[10] R. L. Shriner, E. C. Kleiderer, Org. Synth. 2 (1930) 538.
[11] J. R. Ruhoff, Org. Synth. 2 (1936) 315.
[12] K. Oshima, B. Tollens, Ber. Dtsch. Chem. Ges. 34 (1901) 1425.
[13] H. Fehling, Ann. Chem. Pharm. 72 (1849) 106.
[14] L. T. Sandborn, Org. Synth. 1 (1921) 340.
[15] Q. Tian, D. Shi, Y. Sha, Molecules 13 (2008) 948.
[16] M. Yoshida, Y. Katagiri, W.-B. Zhu, K. Shishido, Org. Biomol. Chem. 7 (2009) 4062.
[17] M. Liu, H. Wang, H. Zeng, C.-J. Li Sci. Adv. 1 (2015) 1500020.
[18] J. Smidt, W. Hafner, R. Jira, J. Sedlmeier, R. Sieber, D. I. R. Rüttinger, D. I. H. Kojer, Angew. Chem. 71 (1959) 176.
[19] G. Zhang, X. Xie, Y. Wang, X. Wen, Y. Zhao, C. Ding, Org. Biomol. Chem. 11 (2013) 2947.
[20] C. N. Cornell, M. S. Sigman, J. Am. Chem. Soc. 127 (2005) 2796.
[21] S. A. C. Carabineiro, Front. Chem. 7 (2019) 702.
[22] A.R. McDonald and L. Que, Jr., Coord. Chem. Rev. 257 (2013) 4357.

[23] L. Que, Jr., Acc. Chem. Res. 40 (2007) 493.

[24] W. Nam, Acc. Chem. Res. 40 (2007) 465.

[25] R. Turcas, D. Lakk-Bogáth, G. Speier, J. Kaizer, Dalton. Trans. 47 (2018) 3248.

[26] R. Turcas, B. Kripli, A.A.A. Attia, D. Lakk-Bogáth, G. Speier, M. Giorgi, R. Silaghi-Dumitrescu, J. Kaizer, Dalton. Trans. 47 (2018) 14416.

[27] E.J. Klinker, J. Kaizer, W.W. Brennessel, N.L. Woodrum, C.J. Cramer and L. Que Jr., Angew. Chem. Int. Ed. 44 (2005) 3690.

[28] J. Kaizer, E.J. Klinker, N.Y. Oh, J.U. Rohde, W.J. Song, A. Stubna, J. Kim, E. Munck, W. Nam and L. Que Jr., J. Am. Chem. Soc. 126 (2004) 472.

[29] Y. Morimoto, J. Park, T. Suenobu, Y.-M. Lee, W. Nam, S. Fukuzumi, Inorg. Chem., 51 (2012) 10025.

[30] C.V. Sastri, M.S. Seo, M.J. Park, K.M. Kim, W. Nam, Chem. Commun. (2005) 1405.

[32] S. Rana, J.P. Biswas, A. Sen, M. Clemancey, G. Blondin, J.-M. Latour, D. Maiti, Chem. Sci. 9 (2018) 7843.

[33] W. Rasheed, A. Draksharapu, S. Banerjee, V.G. Young, Jr., R. Fan, Y. Guo, M. Ozerov, J. Nehrkorn, J. Krzystek, J. Telser, L. Que, Jr., Angew. Chem. Int. Ed. 57 (2018) 9387.

[34] G. Mukherjee, C.W.Z. Lee, S.S. Nag, A. Alili, F.G.C. Reinhard, D. Kumar, C.V. Sastri, S.P. de Visser, Dalton Trans. 47 (2018) 14945.

[35] D. Lakk-Bogath, B. Kripli, B.I. Meena, G. Speier, J. Kaizer, Polyhedron 169 (2019) 169.

[36] B.I. Meena, D. Lakk-Bogáth, B. Kripli, G. Speier, J. Kaizer, Polyhedron 151 (2018) 141.

[37] D. Lakk-Bogath, B. Kripli, B.I. Meena, G. Speier, J. Kaizer, Inorg. Chem. Commun. 104 (2019) 165.

[38] K.-B. Cho, H. Hirao, S. Shaik, W. Nam, Chem. Soc. Rev. 45 (2016) 1197.

[39] D. Lakk-Bogáth, R. Csonka, G. Speier, M. Reglier, A. J. Simaan, J. V. Naubron, M. Giorgi, K. Lazar, J. Kaizer, Inorg. Chem. 55 (2016) 10090.

[40] M. Mitra, H. Nimir, S. Demeshko, S.S. Bhat, S.O. Malinkin, M. Haukka, J. Lloret-Fillol, G.C. Lisensky, F. Meyer, A.A. Shteinman, W.R. Browne, D.A. Hrovat, M.G. Richmond, M. Costas and E. Nordlander, Inorg. Chem. 54 (2015) 7152.

[41] W. Pritzkow, V. Voerckel, H. Weber, J. Prakt. Chem. 335 (1993) 705.

[42] G.A. Russel, J. Am. Chem. Soc. 79 (1957) 3871.

Tel: +36-88-624-720

Fax: +36-88-624-469
e-mail: kaizer@almos.vein.hu

March 03, 2020

Professor C. E. Housecroft
Regional Editor
Polyhedron

Dear Professor **C. E. Housecroft,**

Contribution of authors:
Flóra Viktória Csendes: Reaction kinetics, catalysis studies.
Prof. Dr. József Kaizer: Project leader, writer of the manuscript.

I verify that this submission is original, and that all co-authors are aware of the submission and agree to its publication in the Journal.

Sincerely,
Professor József Kaizer
Department of Chemistry, University of Pannonia
8200 Veszprém
Wartha V. u. 1.
Hungary

Declaration of interests

X The authors declare that they have no known competing financial interests or personal relationships that could have appeared to influence the work reported in this paper.

☐The authors declare the following financial interests/personal relationships which may be considered as potential competing interests:

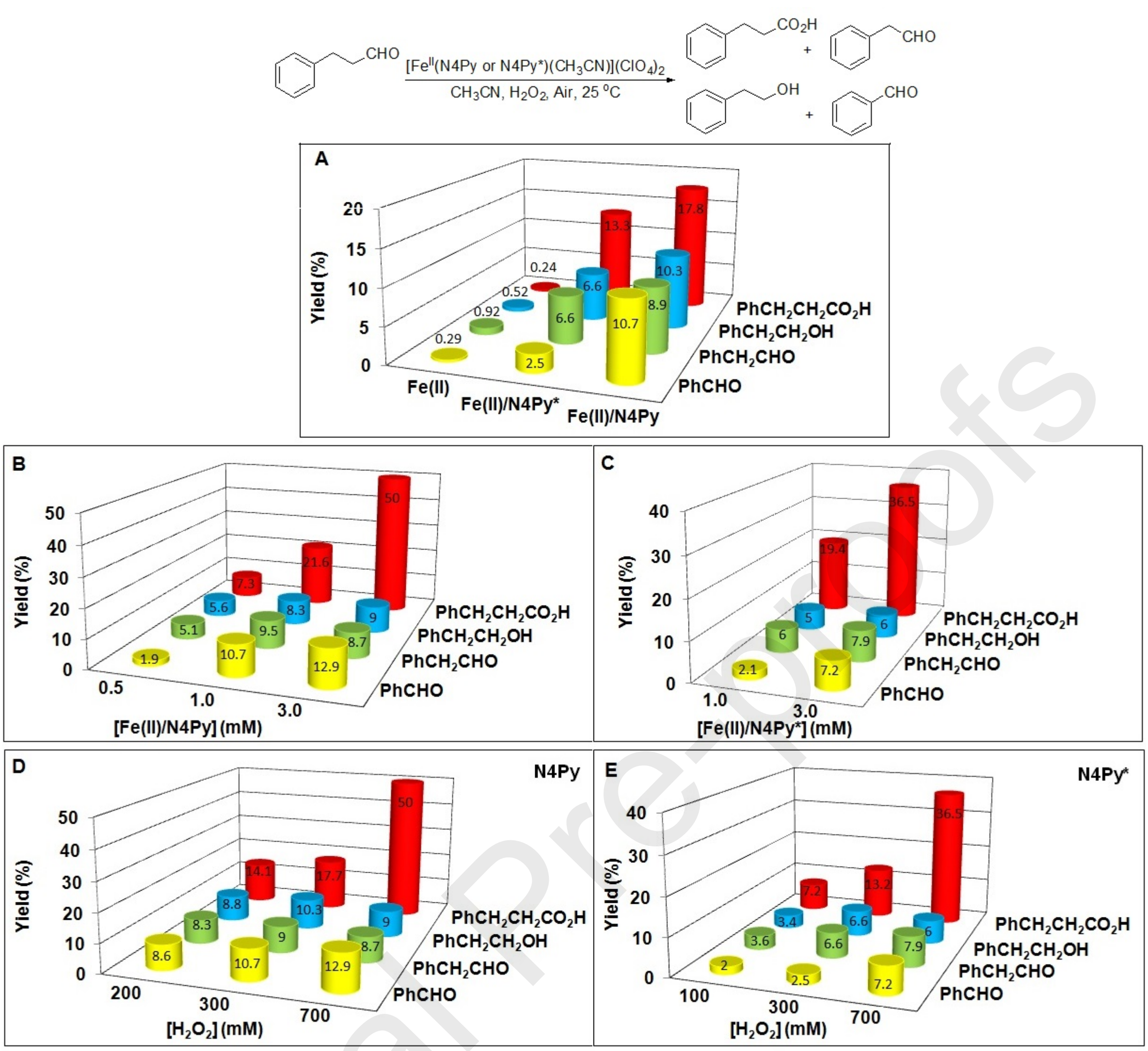
CHO
[Fe^II(N4Py or N4Py*)(CH3CN)](ClO4)2
CH3CN, H2O2, Air, 25 °C
CO2H
+
CHO
OH
+
CHO
A
Yield (%)
0
5
10
15
20
0.29
0.92
0.52
0.24
2.5
6.6
6.6
13.3
10.7
8.9
10.3
17.8
Fe(II)
Fe(II)/N4Py*
Fe(II)/N4Py
PhCH2CH2CO2H
PhCH2CH2OH
PhCH2CHO
PhCHO
B
Yield (%)
0
10
20
30
40
50
1.9
5.1
5.6
7.3
10.7
9.5
8.3
21.6
12.9
8.7
9
50
0.5
1.0
3.0
[Fe(II)/N4Py] (mM)
PhCH2CH2CO2H
PhCH2CH2OH
PhCH2CHO
PhCHO
C
Yield (%)
0
10
20
30
40
2.1
6
5
19.4
7.2
7.9
6
36.5
1.0
3.0
[Fe(II)/N4Py*] (mM)
PhCH2CH2CO2H
PhCH2CH2OH
PhCH2CHO
PhCHO
D
N4Py
Yield (%)
0
10
20
30
40
50
8.6
8.3
8.8
14.1
10.7
9
10.3
17.7
12.9
8.7
9
50
200
300
700
[H2O2] (mM)
PhCH2CH2CO2H
PhCH2CH2OH
PhCH2CHO
PhCHO
E
N4Py*
Yield (%)
0
10
20
30
40
2
3.6
3.4
7.2
2.5
6.6
6.6
13.2
7.2
7.9
6
36.5
100
300
700
[H2O2] (mM)
PhCH2CH2CO2H
PhCH2CH2OH
PhCH2CHO
PhCHO

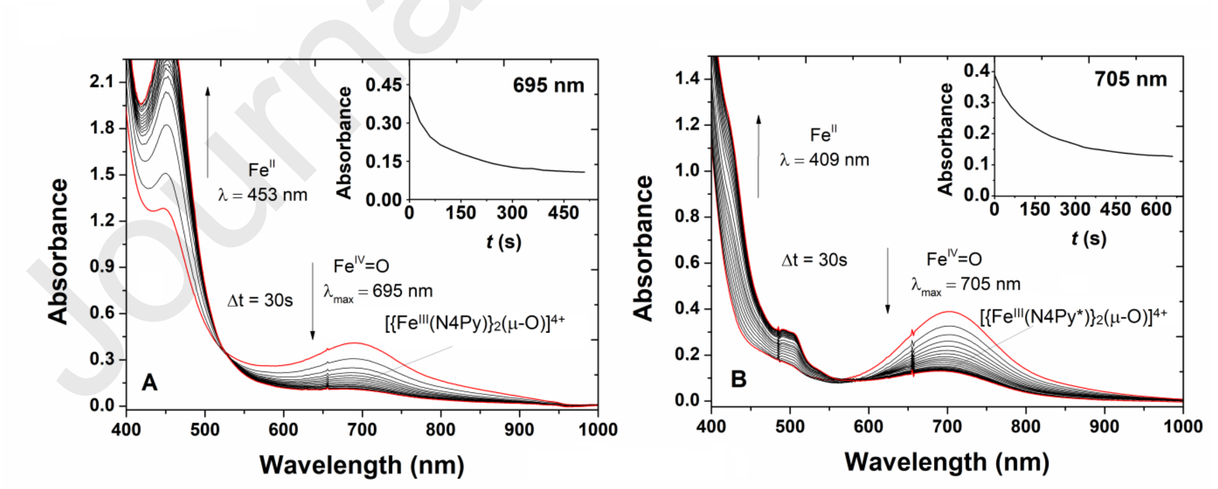
Absorbance
0.0
0.3
0.6
0.9
1.2
1.5
1.8
2.1
Fe^II
λ = 453 nm
Δt = 30s
Fe^IV=O
λmax = 695 nm
[{Fe^III(N4Py)}2(μ-O)]^4+
A
400
500
600
700
800
900
1000
Wavelength (nm)
695 nm
Absorbance
0.00
0.15
0.30
0.45
0
150
300
450
t (s)
Absorbance
0.0
0.2
0.4
0.6
0.8
1.0
1.2
1.4
Fe^II
λ = 409 nm
Δt = 30s
Fe^IV=O
λmax = 705 nm
[{Fe^III(N4Py*)}2(μ-O)]^4+
B
400
500
600
700
800
900
1000
Wavelength (nm)
705 nm
Absorbance
0.0
0.1
0.2
0.3
0.4
0
150
300
450
600
t (s)

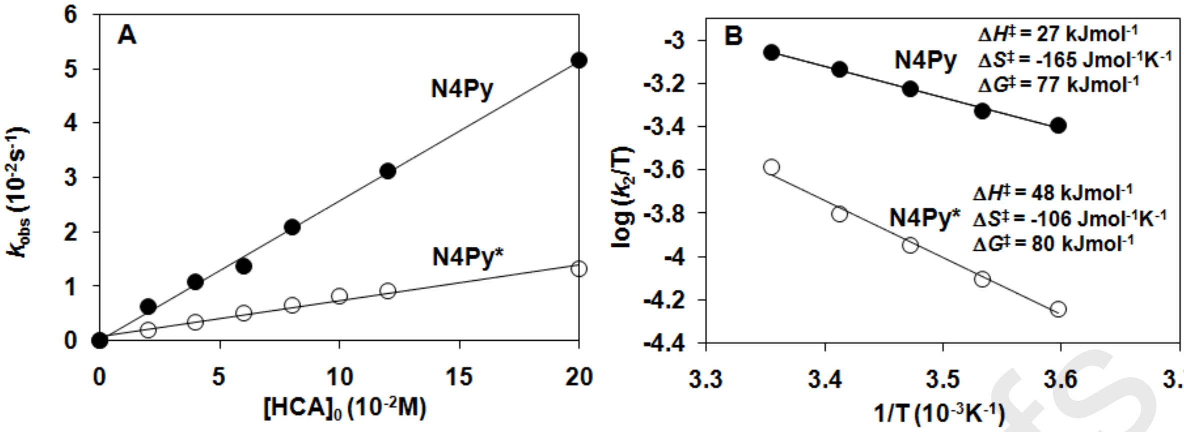
A
k_{obs} ($10^{-2}s^{-1}$)
6
5
4
3
2
1
0
0
5
10
15
20
[HCA]$_0$ (10^{-2}M)
N4Py
N4Py*
B
log (k_2/T)
-3
-3.2
-3.4
-3.6
-3.8
-4
-4.2
-4.4
3.3
3.4
3.5
3.6
3.7
1/T ($10^{-3}K^{-1}$)
N4Py
$\Delta H^‡$ = 27 kJmol^{-1}
$\Delta S^‡$ = -165 Jmol^{-1}K^{-1}
$\Delta G^‡$ = 77 kJmol^{-1}
N4Py*
$\Delta H^‡$ = 48 kJmol^{-1}
$\Delta S^‡$ = -106 Jmol^{-1}K^{-1}
$\Delta G^‡$ = 80 kJmol^{-1}

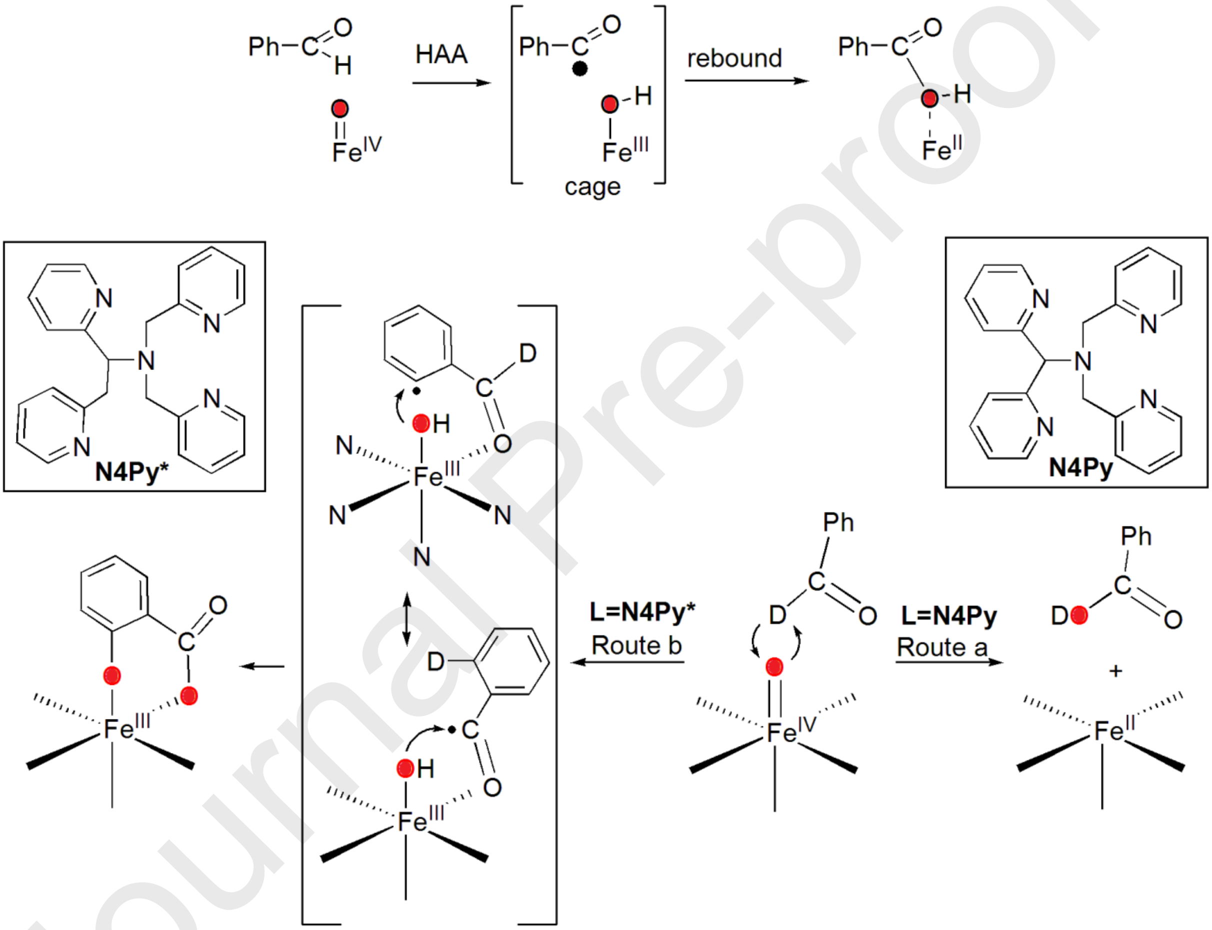
Ph
C
O
H
Fe^{IV}
HAA
cage
Fe^{III}
rebound
Fe^{II}
N4Py*
N4Py
D
N
L=N4Py*
Route b
L=N4Py
Route a
+

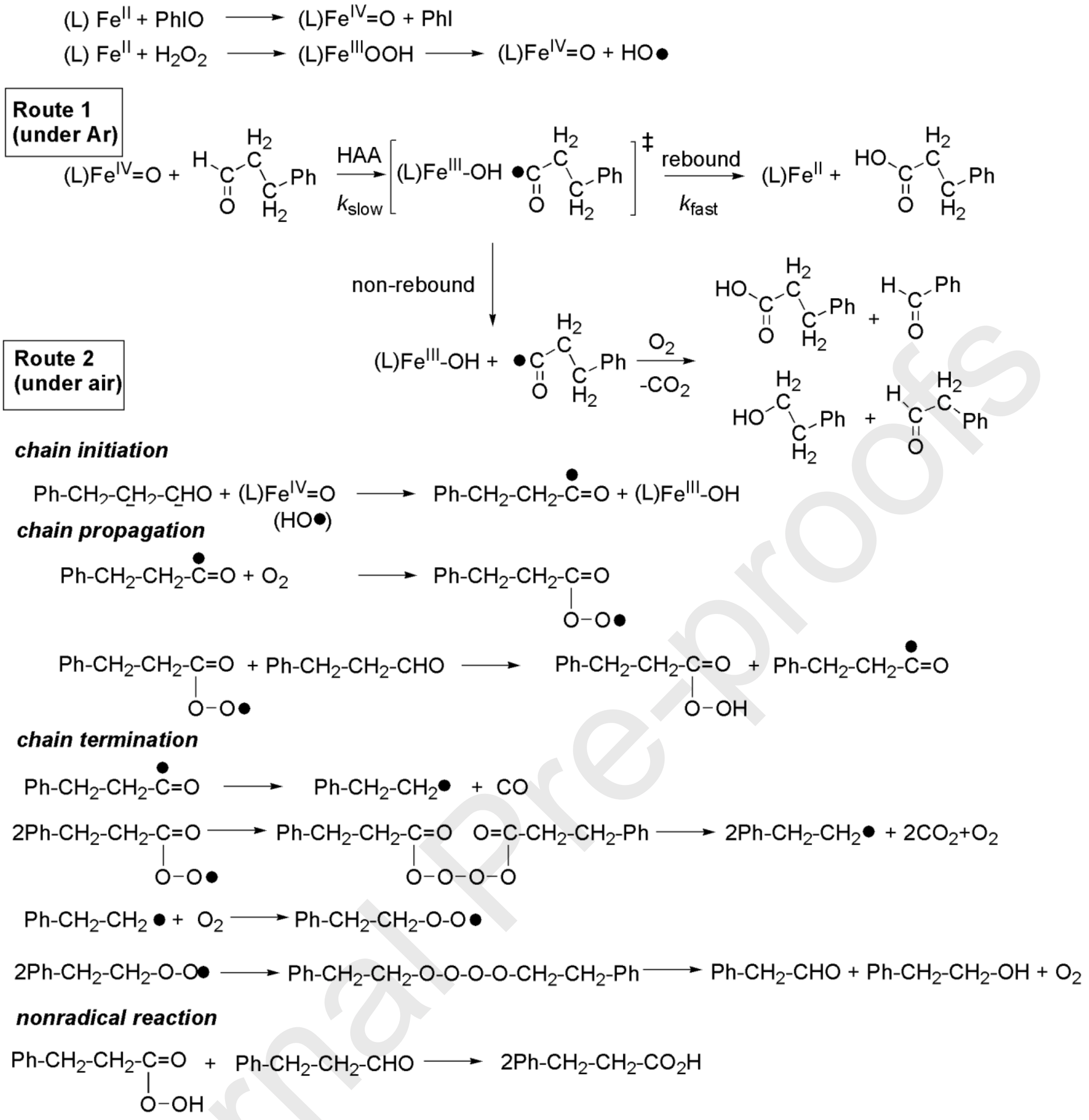

Catalytic and stoichiometric oxoiron(IV) assisted oxidation of hydrocynnamaldehyde under air

Flóra Viktória Csendes and József Kaizer*

Stoichiometric and catalytic oxidation of arylalkyl aldehyde, hydrocinnamaldehyde was investigated by $Fe^{IV}=O$ and their precursor Fe^{II} complexes with H_2O_2 under air to get more insight into the mechanism (RM versus non-RM pathway) of these reactions.

---

*Corresponding author. Tel.: +36 88 62 4720; Fax: + 36 88 62 4469.
E-mail address: kaizer@almos.uni-pannon.hu.

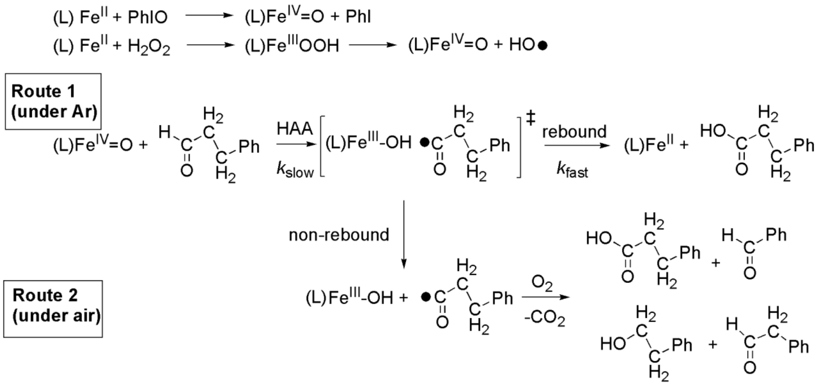
(L) Fe^II + PhIO → (L)Fe^IV=O + PhI
(L) Fe^II + H2O2 → (L)Fe^IIIOOH → (L)Fe^IV=O + HO●
Route 1 (under Ar)
(L)Fe^IV=O +
HAA
kslow
(L)Fe^III-OH
‡
rebound
kfast
(L)Fe^II +
Ph
non-rebound
Route 2 (under air)
(L)Fe^III-OH +
O2
-CO2
HO
H
Ph

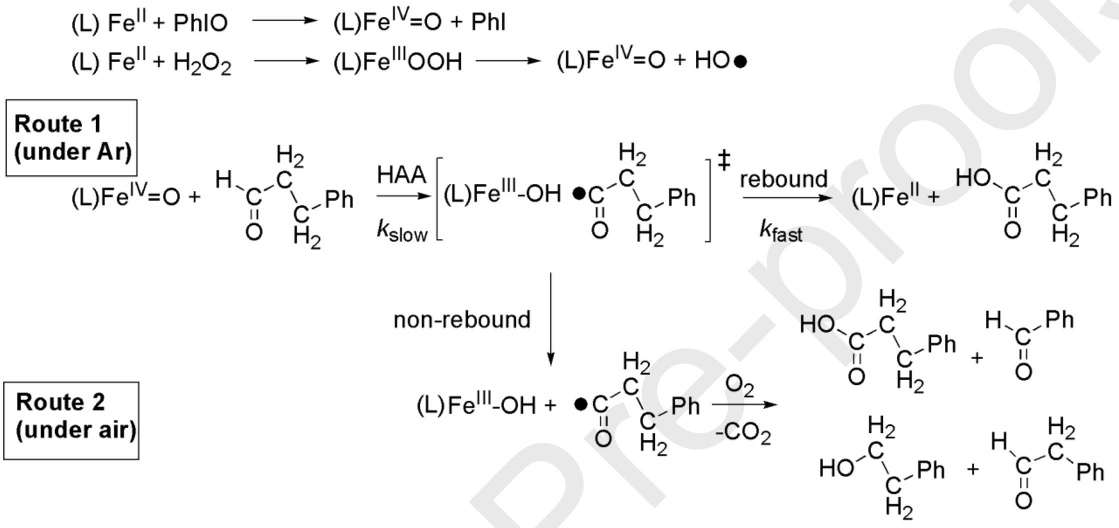
(L) Fe^II + PhIO → (L)Fe^IV=O + PhI
(L) Fe^II + H2O2 → (L)Fe^IIIOOH → (L)Fe^IV=O + HO●
Route 1 (under Ar)
(L)Fe^IV=O +
HAA
kslow
(L)Fe^III-OH
‡
rebound
kfast
(L)Fe^II +
Ph
non-rebound
Route 2 (under air)
(L)Fe^III-OH +
O2
-CO2
HO
H
Ph